LBL-36449
UC-400

Lawrence Berkeley Laboratory
UNIVERSITY OF CALIFORNIA

EARTH SCIENCES DIVISION

Note on the Validity of the Kozeny-Carman Formulas for Consolidated Porous Media

E.M. Schlueter and P.A. Witherspoon

October 1994

REFERENCE COPY
Does Not
Circulate
Bldg. 50 Library.
LBL-36449
Copy 1

Prepared for the U.S. Department of Energy under Contract Number DE-AC03-76SF00098

DISCLAIMER

This document was prepared as an account of work sponsored by the United States Government. While this document is believed to contain correct information, neither the United States Government nor any agency thereof, nor the Regents of the University of California, nor any of their employees, makes any warranty, express or implied, or assumes any legal responsibility for the accuracy, completeness, or usefulness of any information, apparatus, product, or process disclosed, or represents that its use would not infringe privately owned rights. Reference herein to any specific commercial product, process, or service by its trade name, trademark, manufacturer, or otherwise, does not necessarily constitute or imply its endorsement, recommendation, or favoring by the United States Government or any agency thereof, or the Regents of the University of California. The views and opinions of authors expressed herein do not necessarily state or reflect those of the United States Government or any agency thereof or the Regents of the University of California.

LBL-36449
UC-400

Note on the Validity of the Kozeny-Carman Formulas for Consolidated Porous Media*

E.M. Schlueter[†,‡] and P.A. Witherspoon[†]

[†]*Earth Sciences Division*
Lawrence Berkeley Laboratory
University of California
Berkeley, California 94720

and

[‡]*Department of Materials Science and Mineral Engineering*
University of California, Berkeley

October 1994

---

*This research was supported by the U.S. Department of Energy through the Assistant Secretary for Fossil Energy, Bartlesville Project Office, Advanced Extraction Process Technology (AEPT), under contract No. DE-AC22-89BC14475, and by the Director, Office of Energy Research, Office of Basic Energy Sciences, Engineering and Geosciences Division, under Contract No. DE-AC03-76SF00098.

Note on the validity of the Kozeny-Carman formulas for consolidated porous media

E.M. Schlueter[†,‡] and P.A. Witherspoon[†]

[†]*Earth Sciences Division*
Lawrence Berkeley Laboratory
University of California
Berkeley, California, 94720

and

[‡]*Department of Materials Science and Mineral Engineering*
University of California, Berkeley

October 1994

1. Introduction

The simplest and oldest capillaric model is one representing the porous medium by a bundle of parallel straight capillaries of uniform radius. In deriving this Kozeny-Carman model, the multiple connectivity of the pore space is completely neglected. Applying the well-known law of Hagen-Poiseuille for circular tubes of radius r, and relating the result to the macroscopic Darcy's law, it follows that the permeability k of the bundle of capillaries is given by (Scheidegger, 1974)

$$k = \frac{N\pi\bar{r}^4}{8} = \frac{\phi\bar{r}^2}{8}\,, \tag{1}$$

where $\bar{r}$ represents an 'average' pore radius and ϕ the porosity. This model gives permeability in one direction only. All capillaries being parallel, there can be no flow orthogonal to the capillaries. A simple modification to Eq. (1) consists of putting one-third of the capillaries in each of the three spatial dimensions. To account for this, the tortuosity factor, $\tau = 3$, is introduced, and Eq. (1) takes the form

$$k = \frac{N\pi\bar{r}^4}{8\tau} = \frac{\phi\bar{r}^2}{8\tau}\,. \tag{2}$$

The above expression of permeability can be compared with an equation, which determines permeability of sedimentary rocks from microgeometry with reasonable accuracy (Schlueter, 1993). This equation is based on the model of a regular cubic lattice, consisting of pores of different shapes and varying cross sections, and leads to the expression:

$$k = \frac{NC_{eff}}{\tau A_{total}} , \tag{3}$$

where C_{eff} is the effective conductance of the cubic network of coordination number 6, N the number of pore elements in the micrograph, A_{total} the area of the photomicrograph, and τ the tortuosity of a cubic lattice, which is 3. If there are no marked spatial variations of the channel dimensions, the rock is microscopically homogeneous with individual conductances $C_1 = C_2 = ... = C_i = C_{eff} = C$, and the effective conductance becomes independent of the average lattice coordination number z. Hence, under conditions of microscopic homogeneity we can write

$$k = \frac{NC_{eff}}{\tau A_{total}} = \frac{N\frac{1}{2}R_H^2 A}{\tau A_{total}} = \frac{\phi r^2}{8\tau} , \tag{4}$$

where R_H is the ratio of pore area to pore perimeter. Thus, Eq. (3) and Eq. (2) become equivalent. Indeed, the hypothesis of microscopic homogeneity of the pore space is implicit in the derivation of the Kozeny-Carman equations. This would be the case of a rock pore space characterized by a very narrow distribution of channel dimensions, e.g., a single-spike pore-size distribution. However, the pore space of a rock is generally characterized by a wide distribution of channel dimensions, and so the permeabilities predicted by the Kozeny-Carman equation deviates from the measured values. In this case, it will be shown that the Kozeny-Carman formulas based on a parallel arrangement of the pores give at least an upper bound of the rock permeability.

In deriving Eq. (3), a regular cubic lattice, consisting of pores of varying cross sections and different shapes, was introduced as a pore structure model. Permeabilities of sandstones obtained with this model are in good agreement with experimental data (Schlueter, 1993). This outcome confirms previous research by Chatzis and Dul-

lien (1985), who found that the simple cubic (or tetrahedral) networks of angular pores yields very good agreement with the observed data when modeling the mercury porosimetry curve for a variety of sandstones. The simple cubic network and the tetrahedral network were found to give practically indistinguishable results for the mercury porosimetry curve. These results are not surprising when we think that the above properties are strong functions of the pore structure of the sample, which is multiple connected (Figures 1 and 2). On the other hand, consider Berryman and Blair's (1986) estimates of Berea sandstone's permeability using digitized SEM images of rock sections. Parameters such as porosity, specific surface area, and formation factor were employed to successfully predict permeability from Kozeny-Carman relations, and so there seems to be a discrepancy. Therefore, there is a need to assess the region of validity of the Kozeny-Carman formulas to predict permeability of consolidated porous media from microgeometry, as it relates to the microscopic spatial variation of channel dimensions. It is also important to evaluate the extent to which the parallel pore structure model moves away from the regular cubic model as the pore space becomes more and more inhomogeneous at the pore scale. We undertook this research with four main objectives in mind: (1) to re-examine the effective medium theory to treat conductor networks based on the distribution of individual conductances, (2) to study the region of validity of the effective medium theory by comparing its results with conductances evaluated numerically using large 3-D simple cubic networks in which the values of the conductances are chosen by a Monte Carlo procedure from one of several distributions (Kirkpatrick, 1971), (3) to compare results with the critical-path analysis (Ambegaokar et al., 1971) which focuses on the details of the critical paths along which much of the flow must occur (the total conductance obtained by this method gives an upper bound for conductivity valid for the case of having a very broad distribution of channel dimensions, i.e, a microscopically heterogeneous porous medium), (4) to study the validity of the Kozeny-Carman formulas for consolidated porous media as they relate to the microscopic spatial variations of channel dimensions using the effective medium theory, network theory, and the critical path analysis, and ultimately (5) to compare the analytical results thus obtained with experimental results for a variety of consolidated porous materials.

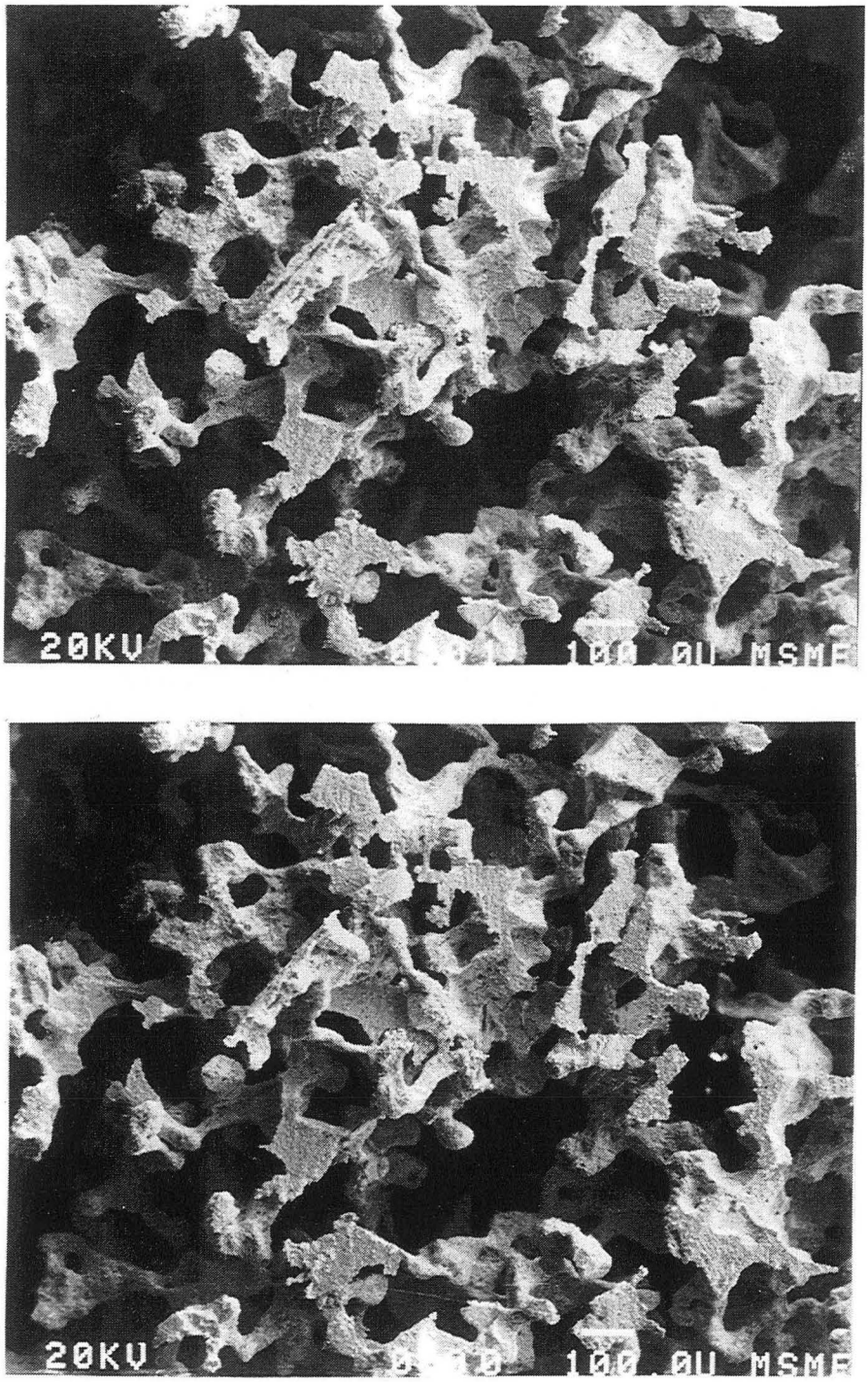

FIG. 1: Stereo SEM photomicrographs of a Berea sandstone pore cast. The rock pore space is partially impregnated with Wood's metal alloy and the quartz grains removed with hydrofluoric acid to reveal the pore microstructure.

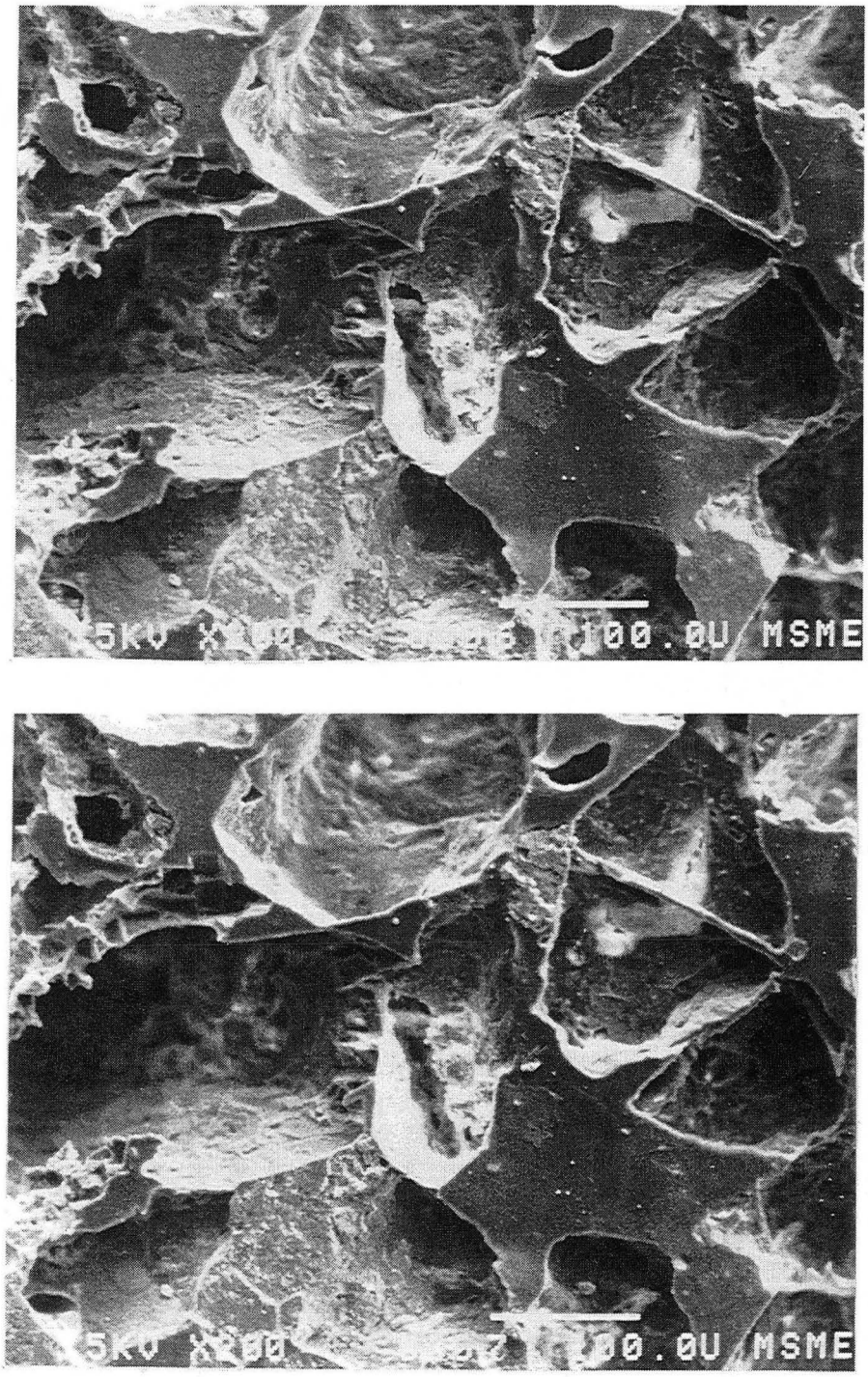

FIG. 2: Stereo SEM photomicrographs of a Saint-Gilles sandstone pore cast. The rock pore space is impregnated with epoxy and the quartz grains removed with hydrofluoric acid to reveal the pore microstructure.

2 Effective medium theory

The objective of the effective medium theory (Kirkpatrick, 1973) is to infer an average conductance parameter for heterogeneous disordered media from the statistics of local conducting elements. Consider an inhomogeneous disordered continuous system in which one can define locally the conductance. Such a medium can be approximated by a 3-D network with a regular topology in which each bond is occuppied by a conductance C_i. According to Kirkpatrick (1973) it is possible to build a homogeneous network with the same topology but in which all conductances C_i have a single value C_{eff} which is an effective value controlling the physical property involved. The effective medium is by definition the homogeneous equivalent network for which the macroscopic conductance is the same as for the heterogeneous system. The idea then, is to represent the average effects of the random conductors by a homogeneous effective medium in which the total field inside is equal to the external field. As a criterion to fix C_{eff} it is required that the incremental voltages induced, where individual conductances C_i are replaced by C_{eff} in this medium, should average to zero.

The distribution of potentials in a random resistor network to which a voltage has been applied along one axis may be regarded as due to both (1) an external field which increases the voltage by a constant amount per row of nodes, and (2) a local fluctuating field whose average over a sufficiently large region is zero.

2.1 *Uniform field solution (external field)*

By introducing a regular cubic mesh of points r_i with spacing Δr (Figure 3), and applying the principle of conservation of charge, one obtains a system of linear equations for the voltages $V_i = V_{r_i}$.

At point i,

$$\sum_j C_{ij}(V_i - V_j) = 0 \,, \tag{5}$$

where j is summed over all neighboring points. Now replacing the conductance C_{ij} with a constant effective conductance C_{eff}, gives at point A (refer to Figure 3)

$$C_{eff}([V + 2V_{eff}]4 - [V + 3V_{eff} + V + V_{eff} + V + 2V_{eff} + V + 2V_{eff}]) = 0 \ , \quad (6)$$

where all conductances C_{eff} have associated with them $\Delta V = V_{eff}$ per row.

2.2 *Fluctuating field solution (local field)*

To find a mathematical expression for the effective conductance, a classical self-consistent method can be employed in which a single conductance C_o is embedded in the homogeneous medium of similar topology. The inclusion of C_o in the effective medium disturbs locally the uniform solution for the field but the deviation is easily calculated since the effective network is homogeneous. Consider one conductance having the value C_o surrounded by an otherwise uniform effective medium. The solution of the network Eq. (5) in the presence of C_o can be constructed by superposition (Figure 4). Far from C_o the field is uniform. To the uniform field solution given by Eq. (6), we add the effects of a fictitious current i_o introduced at A and extracted at B. Since the uniform solution fails to satisfy current conservation at A and B, the magnitude of i_o is chosen to correct for this.

At A,

$$V_{eff}(C_{eff} - C_o) = i_o \ . \quad (7)$$

The extra voltage, V_o, induced between A and B, is given by the conductance C'_{AB} of the network between points A and B when the perturbation is absent, i.e., when $C_o - C_{eff} = 0$:

$$V_o = \frac{i_o}{C_o + C'_{AB}} \ . \quad (8)$$

The current flowing through each of the z equivalent nodes at the point where the current enters is i_o/z so that a total current of $2i_o/z$ flows through the path AB. We then calculate the voltage developed across AB, the conductance across AB, $C_{AB} = (z/2)C_{eff}$, and $C'_{AB} = (z/2)C_{eff} - C_{eff}$.

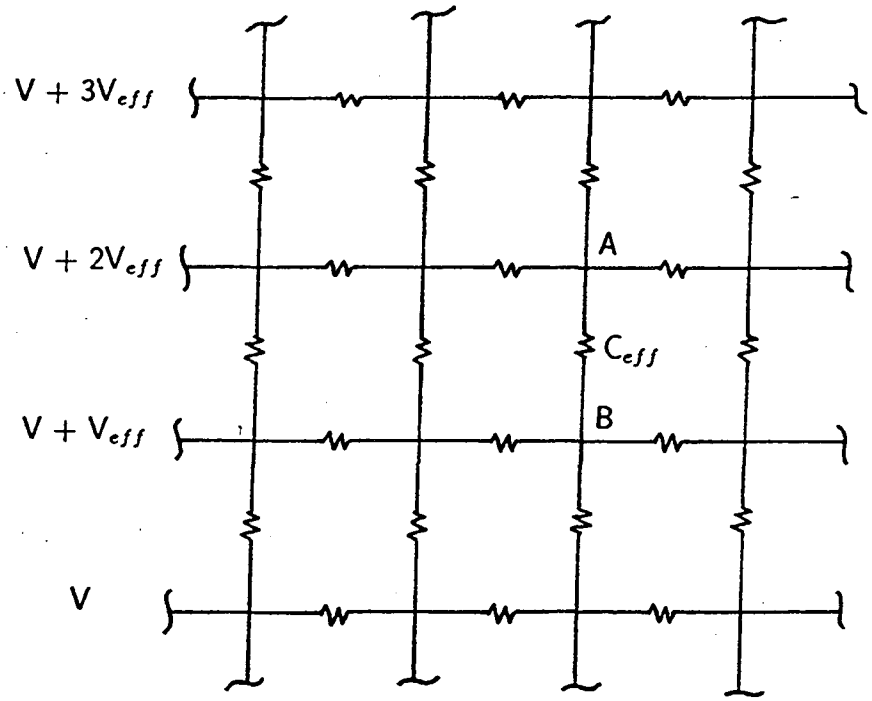

FIG. 3: Construction used in calculating the uniform field solution, in which the voltages increase by a constant amount, V_{eff}, per row.

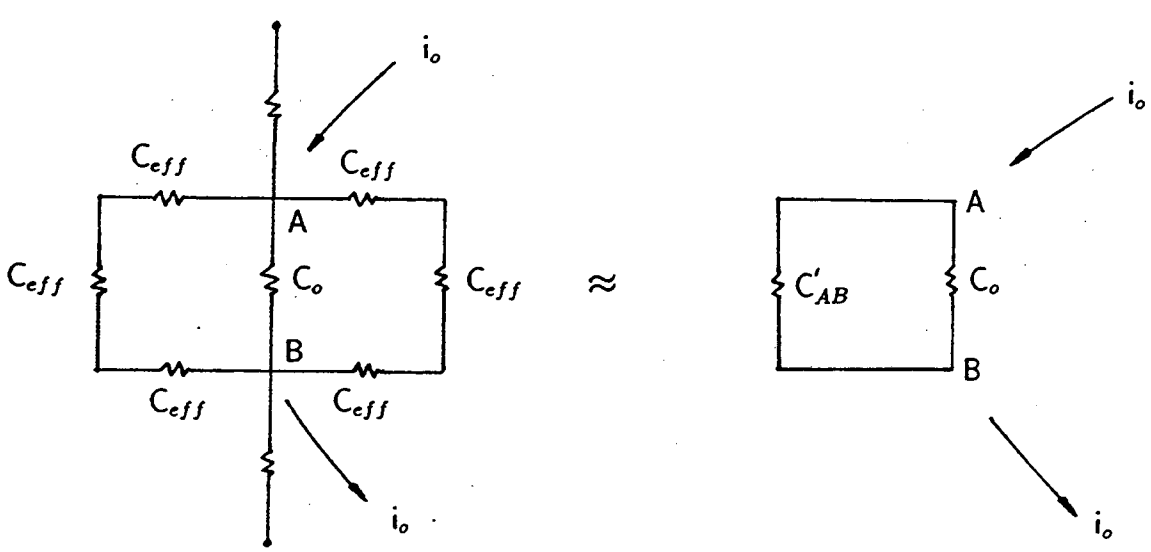

FIG. 4: Construction used in calculating the voltage induced across one conductance, C_o, surrounded by a uniform medium (after Kirkpatrick, 1973).

Thus we can write

$$V_o = \frac{V_{eff}(C_{eff} - C_o)}{C_o + \left[\frac{z}{2} - 1\right] C_{eff}} , \tag{9}$$

valid both in 2-D and 3-D.

The requirement that the average of V_o vanishes gives

$$\left\langle \frac{C_{eff} - C_i}{\left[\frac{z}{2} - 1\right] C_{eff} + C_i} \right\rangle = \sum_{i=1}^{N} \frac{C_{eff} - C_i}{\left[\frac{z}{2} - 1\right] C_{eff} + C_i} = 0 , \tag{10}$$

where the sum is taken over all N individual conductors.

3. Region of validity of the effective medium theory

Evoke the effective medium theory where it was shown that the average effect of a random distribution of conductances in the effective medium can be expressed by giving all conductances a single value C_{eff}, and choosing C_{eff} such that the effects of changing any conductance back to its true value will, on the average, cancel. Changing the value of a conductance located along the electric field from C_{eff} to C_o causes an additional voltage V_o to be induced across C_o given by Eq. (9). If the conductances are distributed according to some distribution function $f(C)$, the self-consistency condition for C_{eff} is

$$0 = \langle V_o \rangle = C_{eff} \int f(C) \left[\frac{C_{eff} - C}{C + (\frac{z}{2} - 1) C_{eff}} \right] dC . \tag{11}$$

Assume a binary distribution of conductances C_{ij}, in which two values C_1 and C_2 occur with probabilities f and $1 - f$, respectively. Applying Eq. (11), we can write

$$f \frac{C_{eff} - C_1}{C_1 + (\frac{z}{2} - 1) C_{eff}} + (1 - f) \frac{C_{eff} - C_2}{C_2 + (\frac{z}{2} - 1) C_{eff}} = 0 . \tag{12}$$

A quadratic equation for C_{eff} is thus obtained

$$\left(\frac{z}{2}-1\right)C_{eff}^2 + C_{eff}\left(C_2\left[\frac{z}{2}(f-1)+1\right] + C_1\left[1-\frac{z}{2}f\right]\right) - C_1C_2 = 0\,. \tag{13}$$

Hence we get

$$\begin{aligned} C_{eff} &= \frac{-C_2\left[\frac{z}{2}(f-1)+1\right] - C_1\left[1-\frac{z}{2}f\right]}{z-2} \\ &\pm \frac{\sqrt{\left(C_2\left[\frac{z}{2}(f-1)+1\right] + C_1\left[1-\frac{z}{2}f\right]\right)^2 - 4\left(\frac{z}{2}-1\right)C_1C_2}}{z-2}\,. \end{aligned} \tag{14}$$

Now let $C_2 \to 0$, in which case C_{eff} becomes

$$C_{eff} = \frac{-C_1\left[1-\frac{z}{2}f\right] \pm C_1\left[1-\frac{z}{2}f\right]}{z-2}\,, \tag{15}$$

with solutions

$$C_{eff_1} = 0\,, \tag{16}$$

and

$$C_{eff_2} = \frac{-2C_1\left[1-\frac{z}{2}f\right]}{z-2}\,. \tag{17}$$

For a simple cubic lattice, $z = 6$, and the non-zero root for C_{eff} becomes

$$C_{eff} = \frac{C_1}{2}[3f-1]\,. \tag{18}$$

Thus

$$\frac{C_{eff}}{C_1} = \frac{3}{2}f - \frac{1}{2}\,. \tag{19}$$

This result is plotted in Fig. 5. Therefore, for $C_2 \ll C_1$, Eq. (19) predicts a linear decrease in C_{eff} with decreasing f, with $C_{eff} \to 0$ when $f \to 1/3$.

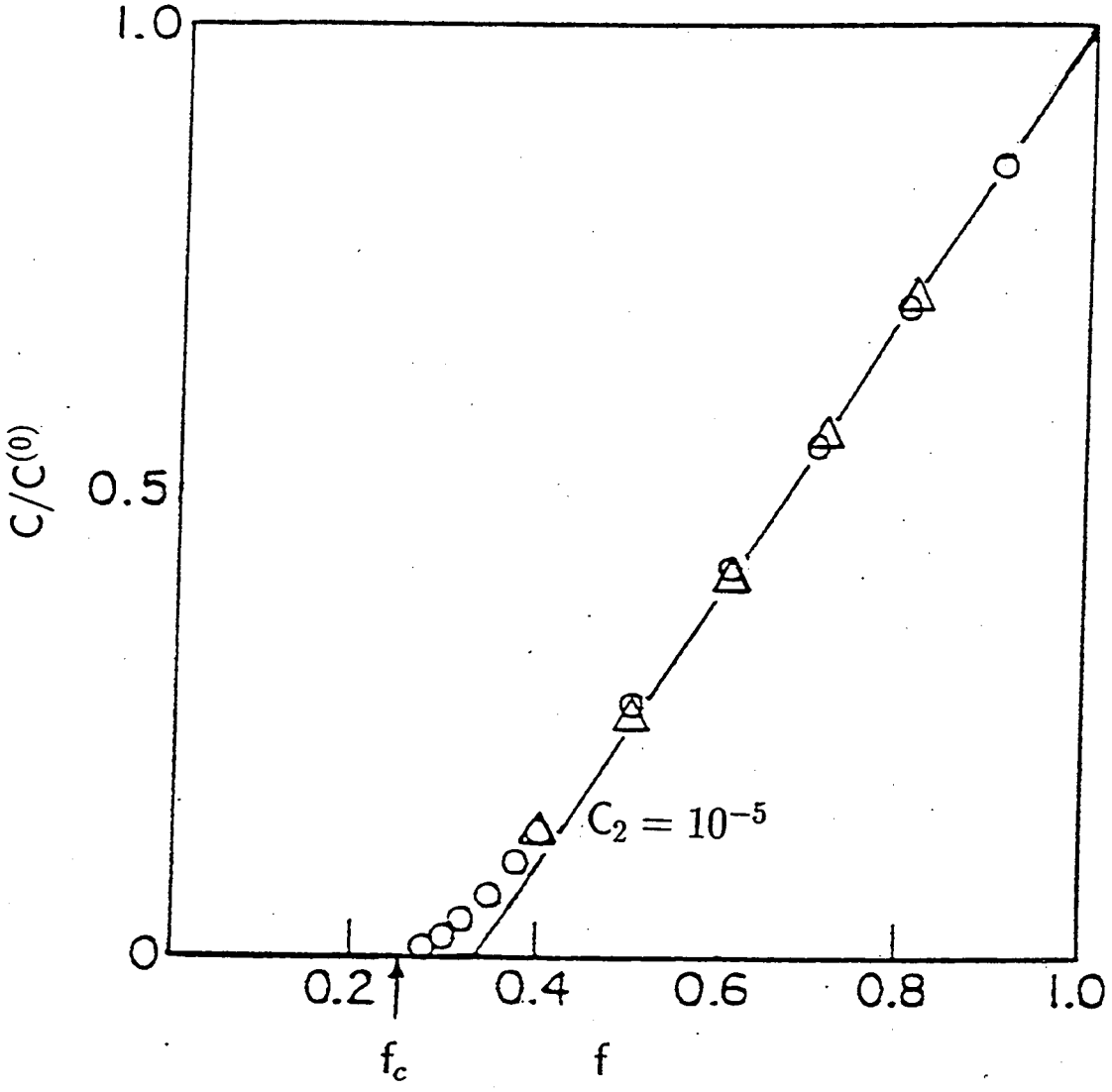

FIG. 5: Total conductance of a simple cubic network of conductances C_{ij} with binary disorder. Values of the conductances are 1 (with probability f) and $C_2 < 1$ (probability $1 - f$), assigned at random. Calculations for networks with 15^3 nodes (data points) and predictions of the effective medium theory (solid line) are displayed. f_c indicates the critical concentration for bond percolation on this lattice (after Kirkpatrick, 1971).

4. Numerical evaluation of the conductances of regular 3-D networks

To study the region of validity of the effective medium theory, Kirkpatrick (1971) evaluated numerically the conductances of large regular 3-D networks, in which the simple cubic values of the conductances (the bonds of the arrays) are chosen by a Monte Carlo procedure from a distribution.

The voltages V_i at the nodes of each network, and from the total current flow for a fixed external applied voltage, were calculated by a relaxation procedure based upon the Kirchhoff current law. If C_{ij} is the conductance of the link between adjacent nodes i and j, the condition that all currents into node i cancel is given by Eq. (5). Resistor networks give a discrete model of a continuous medium in which conductance varies with position. Kirkpatrick (1971) studied the behavior of a simple cubic network of conductances with binary disorder. The values of the conductances are 1 with probability f, and $C_2 \ll 1$ with probability $(1-f)$, assigned at random. Calculations for networks with 15^3 nodes (data points) and predictions of the effective medium theory are given for three values of C_2 in Fig. 5. For $C_2 \ll C_1$ the data shows a linear dependence except in the critical regions where $C_{eff}/C_1 \ll 0.1$ for the binary distribution. Hence, the effective medium theory is expected to work best when the spatial fluctuations in the current (or the channel dimensions) are relatively small. This limit leads to $C_{eff}/C_1 \rightarrow 1.0$. The opposite limit occurs when most of the current is channeled along the paths of least resistance or critical paths along which much of the current will flow. This limit leads to $C_{eff}/C_1 \rightarrow C_c$, where C_c is the critical conductance (section 5). Indeed, the effective medium theory works as long as we are not too close to f_c, the percolation limit.

Kirkpatrick (1971) also calculated conductances of 3-D cubic networks of 15^3 nodes, with values of the conductances chosen at random, distributed uniformily with a distribution $f(C) = (2C \ln A)^{-1}$ and the conductances range from A^{-1} to A, and compared this result with the effective medium theory (Figure 6).

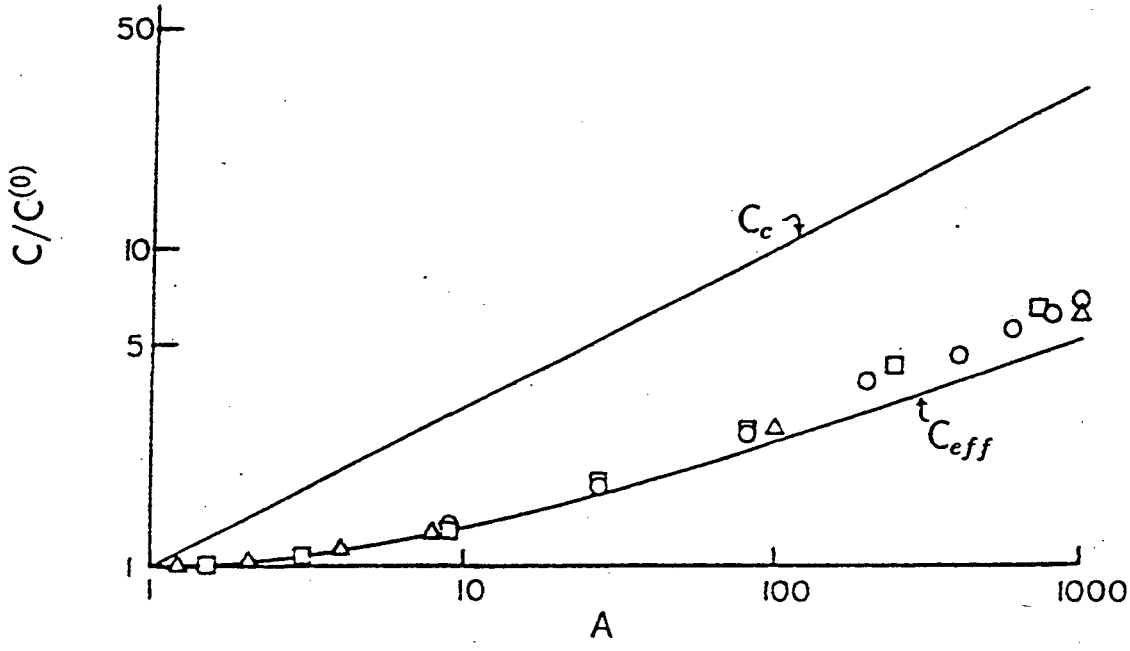

FIG. 6: Symbols show the total conductance of a simple cubic network of 15^3 nodes, with values of the conductances chosen at random from the distribution $f(C) = (2C \log A)^{-1}$ with conductances C_{ij}'s that range from A^{-1} to A. The critical path C_c and the effective conductance C_{eff} have also been plotted (after Kirkpatrick, 1971).

5. Region of validity of the critical path analysis

Ambegaokar et al. (1971) have suggested that most of the current is channeled through the paths of least resistance at low temperatures, in inelastic hopping conduction among localized states. The localized states may be viewed as the nodes i of a random network of conductances C_{ij} with the conductance connecting any two states depending exponentially on the distance between them as well as on their energies. Ambegaokar et al. (1971) suggested that at low temperatures the conductance of such networks, and its temperature dependence, can be estimated by looking at the critical paths, and characterizing them by a critical conductance C_c. The critical conductance can be defined by a simple construction as follows. The resistance network can be considered as composed of three parts (Ambegaokar et al., 1971):

1. A set of isolated 'zones' of high conductance, each region consisting of a group of sites linked together by conductances $C_{ij} \gg C_c$.
2. A relatively small number of conductors with C_{ij} of order C_c, which connect together a subset of the high conductance clusters to form an infinite network that spans the sytem. Conductors in categories (1) and (2) are said to form the 'critical subnetwork'.
3. The remaining conductors with $C_{ij} \ll C_c$.

It is worth noting that in the critical path analysis, the conductances of order C_c determine the conductance of the network. The conductances in category (1) could all be set equal to infinity without greatly affecting the total conductance because the current has to pass through conductances of order C_c to get from one end of the system to the other. The conductances with $C_{ij} \ll C_c$ make a negligible contribution to total conductance because they are effectively shorted out by the critical subnetwork of conductors with $C_{ij} \gg C_c$. Thus the conductances are all removed from the network and then replaced one by one, the largest first. The values of C_{ij} at which extended paths open up is C_c.

Ambegaokar et al. (1971) argue that for a very broad distribution of conductances, as is the case for low temperatures, the conductance may be expressed as

$$C \approx L^{-1} C_c \,, \tag{20}$$

where L^{-1} is less sensitive to the characteristics of the distribution of conductances than is C_c itself. Hence the temperature dependence of C is taken to be of that of C_c alone, the factor L^{-1} adding corrections of order of $\ln C_c$ or less. This analysis yields a very simple and elegant derivation of the $T^{-1/4}$ Mott law for conduction at low temperatures.

The percolation threshold, $f_c = 0.25$, of the numerical bond problem in the 3-D lattice is shown in Fig. 5. This value has also been reported elsewhere (Efros, 1986). If f denotes the ratio of conducting bonds to the total number of bonds, the conductance vanishing at a certain value of f is the threshold (critical) value or percolation threshold. Since $f_c = 0.25$, if the conductances are distributed over the interval (A^{-1} to A) with the weight factor $f(C) = (2C \ln A)^{-1}$, then the critical conductance C_c is easily obtained:

$$f_c \equiv \frac{\int_{C_c}^{A} f(C) dC}{\int_{A^{-1}}^{A} f(C) dC} = \frac{\frac{1}{2 \ln A} \int_{C_c}^{A} \frac{dC}{C}}{1} = 0.25 \,, \tag{21}$$

and

$$C_c = A^{1/2} \,. \tag{22}$$

The critical conductance for such a distribution is plotted in Fig. 6. For the distribution used in the calculation and for the conductances increasing up to $A \approx 1000$, this plot shows that: (1) The effective medium theory and C_{eff} for the simple cubic case only slightly underestimates the observed conductances, and (2) the conduction process is not dominated by the paths of least resistance, and the critical path analysis is immaterial.

6. Region of validity of the Kozeny-Carman formulas and the microscopic spatial variations of channel dimensions

In order to establish the validity of the Kozeny-Carman formulas for consolidated porous media, we will use the effective medium theory and assume that the conductances are distributed according to $f(C) = (2C \ln A)^{-1}$ and that the conductances range from A^{-1} to A. The parallel ($z = \infty$) and the series ($z = 2$) arrangements will be compared to the simple cubic arrangement of the conductors ($z = 6$). In particular, the parallel arrangement (on which Kozeny-Carman formulas are based) will be compared to the simple cubic arrangement of conductors, since the latter was compared with reasonable accuracy to experimental data to calculate permeability of consolidated porous media from microgeometry (Schlueter, 1993). Also, Chatzis and Dullien (1985) have found that the simple cubic network yields results in very good agreement with the experimental data when modeling the mercury porosimetry curve for a variety of sandstones. For comparison purposes, in addition to the effective medium theory results, we plot the observed conductances obtained for a simple cubic arrangement of conductors by Kirkpatrick (1971), and the critical path analysis results in Fig. 7.

6.1. Parallel arrangement of the conductors

For any z we can rewrite Eq. (11) as follows

$$I = \int_{A^{-1}}^{A} \frac{dC}{2C \ln A} \left[\frac{C_{eff} - C}{\frac{C}{z} + \left(\frac{1}{2} - \frac{1}{z}\right) C_{eff}} \right] = 0 \, . \tag{23}$$

For a parallel arrangement of the conductors, $z \to \infty$, and we can write

$$I = \int_{A^{-1}}^{A} \frac{dC}{C} - \frac{1}{C_{eff}} \int_{A_{-1}}^{A} dC = 0 \, . \tag{24}$$

The two integrals can be evaluated to yield

$$\int_{A^{-1}}^{A} \frac{dC}{C} = 2 \ln A \, , \tag{25}$$

and

$$\frac{1}{C_{eff}} \int_{A^{-1}}^{A} dC = \frac{1}{C_{eff}} \frac{A^2 - 1}{A} . \tag{26}$$

Thus, for a parallel arrangement of the conductores, C_{eff} is determined by

$$2C_{eff} \ln A = \frac{A^2 - 1}{A} . \tag{27}$$

Results are plotted in Fig. 7. Clearly, when $A^{-1} = A = 1$, C_{eff} becomes independent of coordination number z.

6.2. Series arrangement of the conductors

For a series arrangement of the conductors, $z = 2$, Eq. (23) gives

$$I = \int_{A^{-1}}^{A} \frac{dC}{2C \ln A} \left[\frac{C_{eff} - C}{C + \left(\frac{2}{2} - 1\right) C_{eff}} \right] = 0 . \tag{28}$$

Thus

$$I = C_{eff} \int_{A^{-1}}^{A} \frac{dC}{C^2} - \int_{A^{-1}}^{A} \frac{dC}{C} = 0 . \tag{29}$$

Solving the two integrals yields

$$C_{eff} \int_{A^{-1}}^{A} \frac{dC}{C^2} = \frac{A^2 - 1}{A} , \tag{30}$$

and

$$\int_{A^{-1}}^{A} \frac{dC}{C} = 2 \ln A . \tag{31}$$

Thus, for a series arrangement of the conductors, C_{eff} is determined by

$$C_{eff} \left[\frac{A^2 - 1}{A} \right] = 2 \ln A . \tag{32}$$

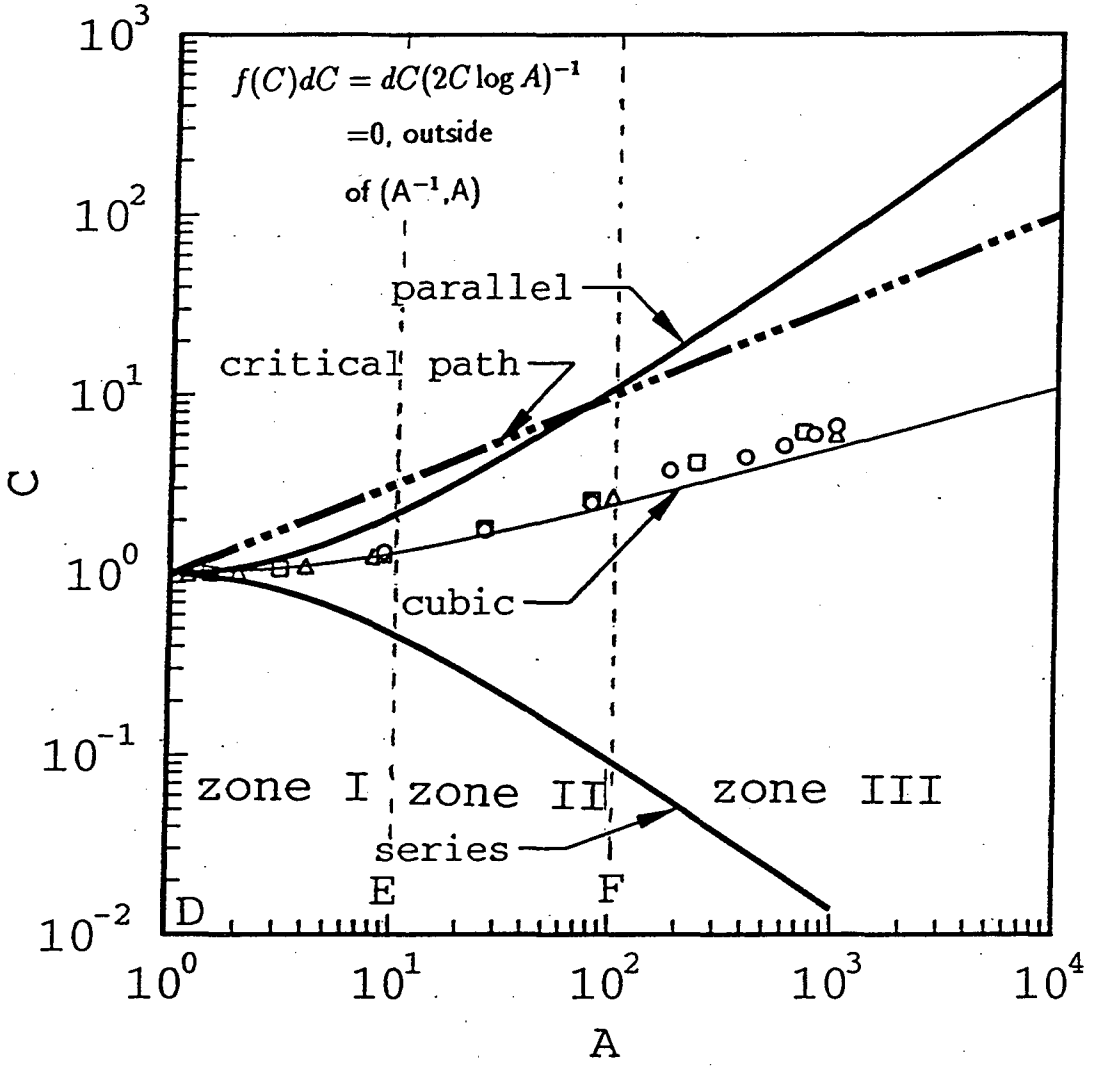

FIG. 7: Effective conductances of a parallel, simple cubic, and series networks of conductors, with values of the conductances chosen at random from the distribution $f(C)$ indicated. The critical path conductance and the total conductance of a simple cubic network from previous figure (data points) have also been plotted. Zones I, II, and III correspond to zones within which the Kozeny-Carman formulas are valid, approximately valid, and not valid, respectively.

Results are plotted in Fig. 7. Clearly, as $A^{-1} = A \to 1$, C_{eff} approaches independency of coordination number z.

6.3. Simple cubic arrangement of the conductors

For a simple cubic lattice, $z = 6$, Eq. (23) gives

$$I = \int_{A^{-1}}^{A} \frac{dC}{2C \ln A} \left[\frac{C_{eff} - C}{C + \left(\frac{6}{2} - 1\right) C_{eff}} \right] = 0 \,. \tag{33}$$

Thus

$$I = \int_{A^{-1}}^{A} \frac{C_{eff} dC}{C(C + 2C_{eff})} - \int_{A^{-1}}^{A} \frac{dC}{C + 2C_{eff}} = 0 \,. \tag{34}$$

Solving the partial integrals

$$\int_{A^{-1}}^{A} \frac{C_{eff} dC}{C(C + 2C_{eff})} = -\frac{1}{2} \left[\ln \frac{2C_{eff} + A}{2C_{eff} + A^{-1}} - 2 \ln A \right] \,, \tag{35}$$

and

$$\int_{A^{-1}}^{A} \frac{dC}{C + 2C_{eff}} = \ln \frac{A + 2C_{eff}}{A^{-1} + 2C_{eff}} \,. \tag{36}$$

Thus C_{eff} for a simple cubic lattice is determined by

$$3 \ln \frac{2C_{eff} + A}{2C_{eff} + A^{-1}} = 2 \ln A \,. \tag{37}$$

Results are plotted in Fig. 7. Evidently, as $A^{-1} = A \to 1$, C_{eff} approaches independency of coordination number.

The solution to Eq. (37) for $A \to \infty$ is readily obtained:

$$3 \ln \frac{2C_{eff} + A}{2C_{eff}} = 3 \ln A - 3 \ln 2C_{eff} = 2 \ln A \,, \tag{38}$$

and

$$C_{eff} \approx \frac{1}{2} A^{1/3} . \tag{39}$$

For very large A, the data falls approximately on a straight line of slope $\sim 1/3$.

5.4. Results and discussion

Figure 7 shows a log-log plot of C_{eff} for the parallel, series, and the cubic arrangements, respectively. For comparison purposes, in addition to the effective medium theory results, we have plotted the critical path analysis results and the results obtained by Kirkpatrick (1971) for a simple cubic arrangement of conductors. In particular, the parallel arrangement will be compared to the simple cubic arrangement of conductors, since the latter was tested with reasonable accuracy against experimental data to calculate permeability of consolidated porous media from microgeometry (Schlueter, 1993). This result simply confirmed previous findings by Chatzis and Dullien (1985) when modeling the mercury porosimetry curve for sandstones. For the distribution used in the calculation and for the range of conductances increasing up to $A \approx 1000$, this plot shows that: (1) C_{eff} for the simple cubic case only slightly underestimates the observed conductances, (2) C_{eff} for the series case provides a lower bound for the observed conductances, (3) C_c is the upper most bound for the observed conductances up to $A \approx 70$, whereas C_{eff} for the parallel case is the upper most bound thereafter, and (4) the conduction process is not dominated by the paths of least resistance, making the critical path analysis irrelevant.

To explore the region of validity of the Kozeny-Carman formulas, we have utilized the conductance envelope for the given distribution of conductances (Fig. 7), and divided it into three zones: zone I ($1 < A < 10$), a zone within which the Kozeny-Carman formulas are valid; zone II ($10 \leq A \leq 100$), a zone within which the Kozeny-Carman formulas are approximately valid within limits; and zone III ($A > 100$), a zone within which the Kozeny-Carman formulas are not valid. Zone I, in which conductance span A varies between limits 1 (point D) and 10 (point E), is characterized by conductances C_{eff} for the parallel case being less than two times higher than the cubic case over much of the conductance span. In this zone, the Kozeny-Carman relations are valid within experimental error. Consider, for exam-

ple, that in the analytical expression for permeability given by Eq. (3), the error incurred in the hydraulic radius approximation lies within ±30%. Notice that point D corresponding to the limit $A = 1 = A^{-1}$ is associated with the point at which $C_{eff} = 1$. Therefore, at point D, the porous medium is microscopically homogeneous, and the Kozeny-Carman formulas are strictly valid. In zone I, the spatial fluctuations in channel dimensions are small and the Kozeny-Carman formulas are very accurate. Notice also, that in this zone the critical path conductance C_c provides an upper most bound, and C_{eff} for the series case ($z = 2$) provides a lower bound. Zone II, in which conductance span A varies between limits 10 (point E) and 100 (point F), is characterized by conductances C_{eff} for the parallel case being less than an order of magnitude higher than the simple cubic case. Since the permeability of rocks can range over many orders of magnitude, from about 10^{-11} m^2 down to about 10^{-20} m^2, an estimation of permeability within less than an order of magnitude of the observed value may be sufficient for many practical applications. However, in this zone the pore system is, strictly speaking, microscopically inhomogeneous. Zone II is a transition zone regarding the upper bound conductance because when $A \approx 80$, C_{eff} for the parallel case becomes the upper bound conductance. C_{eff} for the series case provides of a lower bound conductance during the whole span. Zone III, in which conductance span A varies between limits 100 (point F) and higher is characterized by conductances C_{eff} for the parallel case being more than order of magnitude higher than the simple cubic case. At this stage, the pore system is considered highly inhomogeneous. Notice that C_{eff} for the parallel case is here the upper most bound. The critical path conductance, C_c, is accurate only to within an order of magnitude.

7. Comparison of analytical and experimental results

The analytical results for permeability calculated in the manner described above will now be (1) compared against analytical and experimental results for sandstones obtained by Chatzis and Dullien (1985), (2) compared with analytical and experimental results for sandstones obtained previously (Schlueter, 1993), and (3) analyzed in light of the mercury porosimetry experimental data for a variety of sandstones obtained by Batra (1973).

As shown in earlier work (Schlueter, 1993), our permeability model was able to

predict the property for a variety of sandstones while using, in every case, the same cubic lattice as the pore-structure. Chatzis and Dullien (1985) also introduced a regular cubic lattice, consisting of capillary tubes of uniform, but angular cross section, at the intersections of which are angular bulges. Drainage-type penetration numerical experiments were performed in a number of regular networks representing the pore space, using a modified site-percolation approach. All of their networks are composed of two topological entities: capillaries and nodes. The correlation between the probability of a capillary being open and that of a node being open is considered in the calculation. From these results the porosimetry curve of mercury in sandstones, the relative permeability curve of mercury in sandstones, and the relative permeability curve of oil in a sandpack were calculated. The physical basis of the calculations is a one-to-one correspondence between the probability of a capillary being open, and the cumulative distribution function of capillary diameters. Capillaries and bulges are characterized by size distribution functions, and the bulges of different sizes are distributed randomly over the nodal points (sites) of the network. The choice of the size of a capillary is limited by the condition that it may not exceed the size of either of the two bulges located at the two ends of the capillary. In the calculations, realistic capillary and node diameter distribution functions, pore shapes and relationships between the volume and the diameter of a pore were assumed. In their model, however, the aspect of the pore structure called 'geometry', such as the dimensions and the orientation of the pores, are not modeled. The simple cubic (or tetrahedral) network was found to give results in good agreement with the experimental data (Fig. 8).

The angular bonds (pore throats) correspond to pores of diameter D_b. Consistency with the customary definition of pore size used in mercury porosimetry, with the aid of the well-known relationship of Laplace, enables Chatzis and Dullien (1985) to define the capillary diameters as follows

$$D_{b_k} = 2R_{b_k} \cos\theta \ , \tag{40}$$

where R_{b_k} is the radius of curvature of the meniscus of the nonwetting phase at the prevailing capillary pressure, θ is the contact angle, and D_{b_k} is the diameter of capillary k.

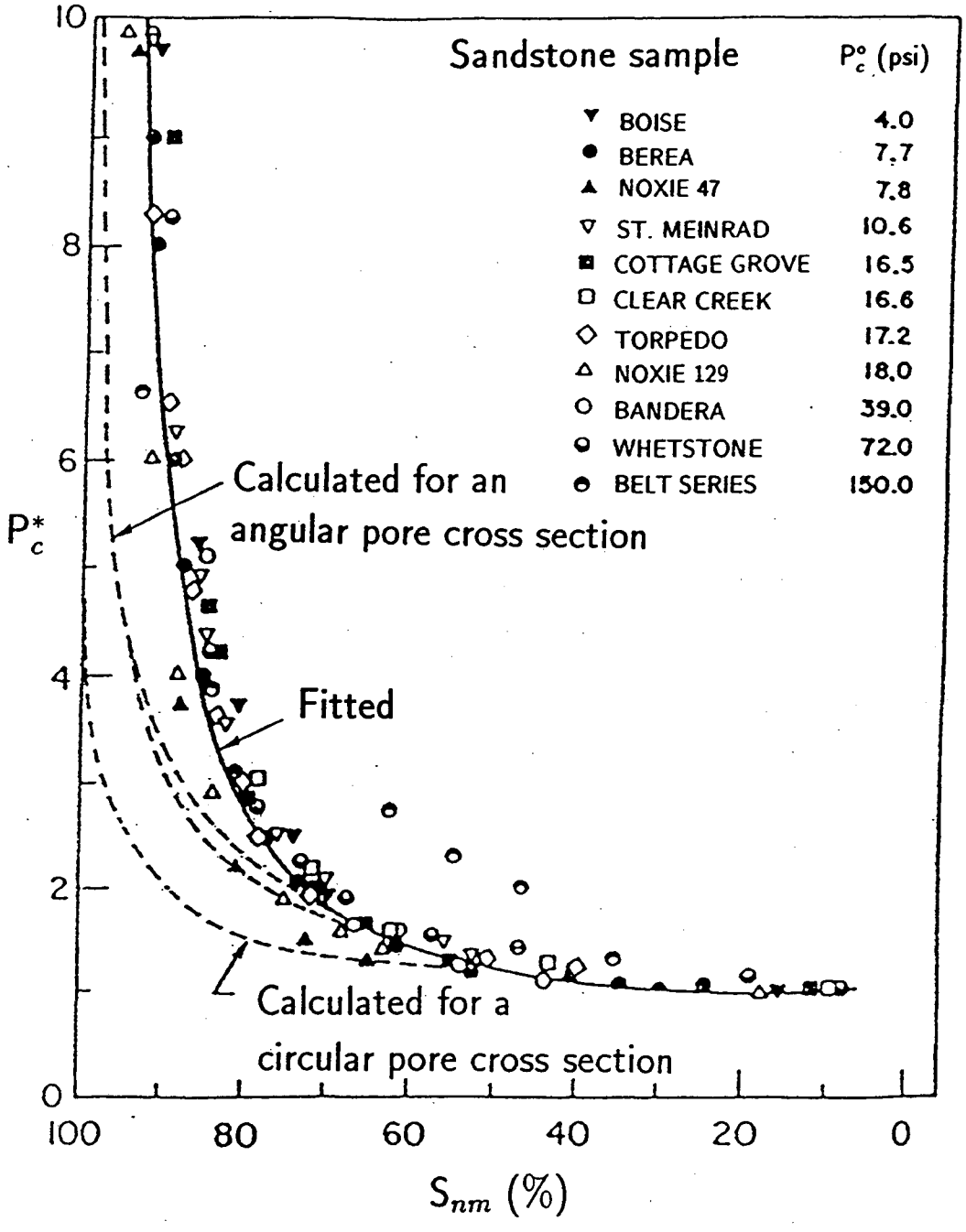

FIG. 8: Dimensionless experimental mercury-porosimetry data and analytical curve of sandstone samples. A regular cubic lattice consisting of capillary tubes of angular cross section, at the intersections of which there are angular bulges, is introduced as a pore structure model. The experimental data for all of the sandstone samples (except Belt Series) are well fitted by a single curve (solid line). The capillary pressure is normalized to the breakthrough capillary pressure P_c^o (after Chatzis and Dullien, 1985).

TABLE 1: Calculation of the mercury porosimetry curve of the Berea (BE-1) sandstone sample (after, Chatzis and Dullien, 1985).

P^*_{ck}	D_{b_k}	$D^2_{b_k} f_b$	D_{s_k}	$D^2_{s_k} f_s$	S^*_{nmk}	S^o_{nmk}
1.00	29.5	102.3	44.5	848.0	0.113	0.170
1.02	28.8	104.9	44.0	843.8	0.164	0.252
1.09	27.0	109.5	42.5	826.3	0.286	0.415
1.15	25.5	110.6	41.0	802.1	0.365	0.519
1.23	24.0	109.4	39.5	771.8	0.443	0.599
1.32	22.4	105.6	38.0	735.9	0.496	0.667
1.43	20.7	99.1	37.0	709.2	0.552	0.724
1.54	19.2	91.4	35.5	665.3	0.605	0.776
1.68	17.6	81.6	34.0	617.0	0.659	0.824
1.84	16.0	70.6	33.0	582.6	0.708	0.862
2.06	14.3	58.1	31.5	527.6	0.764	0.902
2.36	12.5	44.7	30.0	468.3	0.818	0.937
2.78	10.6	31.1	28.5	403.1	0.869	0.965
3.47	8.5	17.8	27.0	327.5	0.918	0.987
5.90	5.0	0	25.0	0	0.972	1.000

Analogously, for pores (pore bodies) of diameter D_{s_k}:

$$D_{s_k} = 2R_{s_k} \cos\theta \ , \tag{41}$$

where R_{s_k} is the radius of curvature of the meniscus of the nonwetting phase at the prevailing capillary pressure, θ is the contact angle, and D_{s_k} is the diameter of pore k.

Table 1 (Chatzis and Dullien, 1985) gives the calculated values of the mercury porosimetry curve of the Berea (BE-1) sandstone sample using a cubic lattice of non-circular (and circular) pores. Berea (BE-1) sandstone has almost the same macroscopic transport properties as the Berea sandstone used in our experiments (i.e., porosity of 22%, permeability to N_2 of 400 md, and a formation factor of 15.5). The capillary pressure P^*_{ck} is given relative to the breakthrough pressure P^o_c. The diameters of the pores D_{b_k}, and D_{s_k} were calculated for the prevailing capillary pressure and its corresponding saturation. The density functions $f_b(D_b)$ and $f_s(D_s)$ were assumed to be given by the beta function. The saturations $S^*_{nm_k}$ and $S^o_{nm_k}$ are the saturations of the angular and circular pore networks, respectively.

To compare our analytical calculations for permeability obtained above with the

results obtained by Chatzis and Dullien (1985) for Berea (BE-1), we need first to relate the diameter D_k of each angular pore to its individual hydraulic conductance C_k. Schultze (1925a, b) has shown that the capillary pressures for noncircular capillaries under the assumption of zero contact angle are given by

$$P_c = \frac{\epsilon}{R_H}\,; \quad \frac{1}{R_H} = \frac{1}{r_1} + \frac{1}{r_2}\,, \tag{42}$$

where ϵ is the surface tension, r_1 and r_2 the principal radius of curvature, and R_H the hydraulic radius as defined previously. For an equilateral triangle of side a, the equivalence of the reciprocal of the hydraulic radius and the reciprocal mean radius of curvature is (Carman, 1941)

$$\frac{1}{R_H} = \frac{1}{r_1} + \frac{1}{r_2} = \frac{2}{R_k} = \frac{4}{D_k}\,. \tag{43}$$

Thus, at zero contact angle, D_k and R_H are related. The area A and the perimeter P of the equilateral triangular pore are $\sqrt{3}a^2/4$ and $3a$, respectively. The hydraulic radius is $R_H = A/P = \sqrt{3}a/12$, and the pore diameter is $D_k = \sqrt{3}a/3$. Therefore, the angular pore area in terms of the diameter D_k is $A = 3\sqrt{3}D_k^2/4$.

Recall the equation used earlier for calculating the individual pore conductances (Schlueter, 1993)

$$C_k = \frac{1}{2}R_H^2 A\,. \tag{44}$$

In terms of pore diameter D_k, and under the assumption of zero contact angle, the pore conductance becomes

$$C_k = \frac{3\sqrt{3}}{128}D_k^4\,. \tag{45}$$

Table 1 (Chatzis and Dullien, 1985), gives the calculated pore diameters D_k for Berea sandstone (BE-1) for the full range of capillary pressures and saturation. At this stage, we need to calculate the pore conductances of the 'primary' pore network which is the one accountable for hydraulic transport. Our experimental results have

consistently shown that the hydraulically active or 'primary' pore network in sandstones consists of intergranular pores (bodies and throats), situated in between the grains (Schlueter et al., 1994). The hydraulically active or 'primary' network of intergranular pores in Berea sandstone comprises about 80% of the total rock porosity. About 20% of the total rock porosity consists of grain contact pores; both inside the cementing material, and a few between grains when the pore has been narrowed down by deposits to a very narrow gap. Since the contribution of the grain-contact or 'secondary' network to hydraulic transport is small, it can therefore be considered hydraulically inactive (Schlueter et al., 1994). The pore (pore throat) diameters of the 'principal' network of Berea sandstone range from the critical diameter $D_c = 29.5$ μm corresponding to the breakthrough pressure P_c^o (and corresponding saturation $S^*_{nm_k} = 0.113$) to the value $D_{b_k} = 12.5$ μm (and corresponding saturation $S^*_{nm_k} = 0.80$). The breakthrough diameter $D_c = 29.5$ μm is the largest diameter of the first connected cluster that spans the whole sample. On the other hand, the pore diameter $D_{b_k} = 12.5$ μm is the minimun diameter of the 'principal' network, consisting of intergranular pores, i.e., in between grains. From the 'principal' network of Berea sandstone (BE-1), the maximum and minimum pore diameters are thus obtained, and the ratio of critical to minimum pore conductances calculated with the aid of Eq. (43) is:

$$\frac{C_c}{C_{min}} = \frac{D_c^4}{D_{min}^4} = \frac{29.5^4}{12.5^4} \approx 31 \ . \tag{46}$$

Using the C_c/C_{min} ratio for Berea sandstone, it is then possible to go to the general conductance plot (Figure 7) and obtain the ratio of effective conductance for the parallel case ($z = \infty$) to the effective conductance for the cubic case ($z = 6$)

$$\frac{C_{eff_{parallel}}}{C_{eff_{cubic}}} \approx 3 \ . \tag{47}$$

The above result is consistent with previous calculations on permeability of Berea sandstone presented elsewhere (Schlueter, 1993). For example, conductance calculations for Berea sandstone section B (Table 2), using the effective medium theory in conjunction with the 'principal' pore network, gave effective conductances for the parallel case ($z = \infty$) and for the cubic case ($z = 6$) such that their ratio is given by

TABLE 2: Calculated effective conductance data of various sandstones obtained from SEM 2-D sections (Schlueter, 1993).

Rock	C_{eff} $(z^* = \infty)$ m^4	C_{eff} $(z^* = 6)$ m^4	$\frac{C_{eff}\ (z^*=\infty)}{C_{eff}\ (z^*=6)}$
Berea sandstone B	56.0×10^{-20}	18.2×10^{-20}	3.1
Berea sandstone T	59.9×10^{-20}	24.2×10^{-20}	2.5
Boise sandstone	$80.1\ \times10^{-20}$	45.0×10^{-20}	1.8
Massilon sandstone	525×10^{-19}	90.7×10^{-19}	5.8
Saint-Gilles sandstone	48.3×10^{-20}	21.2×10^{-20}	2.3

*Coordinatiom number.

TABLE 3: Calculated permeability data of two sandstones from rock microgeometry assuming a parallel pore model (Schlueter, 1993).

Rock	k $(z^* = \infty)$ m^2	$k_{measured}$ m^2	$\frac{k\ (z^*=\infty)}{k_{measured}}$
Berea sandstone B	15.0×10^{-13}	4.8×10^{-13a}	3.1
Massilon sandstone	10.8×10^{-12}	2.5×10^{-12b}	4.3

[a]Distilled water used as permeant.
[b]Data from Koplik et al., 1984.

$$\frac{C_{eff_{parallel}}}{C_{eff_{cubic}}} = \frac{56.0 \times 10^{-20}\ m^4}{18.2 \times 10^{-20}\ m^4} \approx 3\ . \tag{48}$$

Analogously, for Berea sandstone section T (Table 2), the effective medium theory in conjunction with the 'principal' network gave effective conductances such that their ratio is

$$\frac{C_{eff_{parallel}}}{C_{eff_{cubic}}} = \frac{59.9 \times 10^{-20}\ m^4}{24.2 \times 10^{-20}\ m^4} \approx 3\ . \tag{49}$$

Similarly, former research summarized in Table 3 (Schlueter, 1993), showed that a model based on the 'principal' pore network, a parallel arrangement, and a pore size distribution, gave the permeability for Berea sandstone section B such that its ratio to the observed value is

$$\frac{k_{parallel}}{k_{measured}} = \frac{15.0 \times 10^{-13}\ m^2}{4.8 \times 10^{-13}\ m^2} \approx 3\ . \tag{50}$$

It is then concluded that Berea sandstone hydraulically active conductances fall into zone II of Fig. 7, and that the Kozeny-Carman relations are valid within a factor of three of the measured permeability values. But, how general is this result for most sandstones, especially considering that the range of pore diameters may vary widely from one rock to another? This issue becomes quite clear when one examines the normalized experimental capillary pressure curves shown in Fig. 8 for a variety of sandstones. They almost without exception can be represented by a single function (solid line). This is a direct consequence of the 'similarity' in the geometrical sense of the pore structure and of the 'principal' pore network of ten of the eleven sandstone samples under study. The absolute magnitudes of the pore sizes alone do not determine the results of these calculations. It is the pore diameters and pore conductances of the hydraulically active pore network, relative to the breakthrough pore diameter and corresponding conductance, rather than the absolute magnitudes of the pore diameters and corresponding conductances of the complete network, that determine the permeability and capillary pressure results. The successful prediction of permeability from microgeometry (Schlueter, 1993), and of the mercury porosimetry curve by Chatzis and Dullien (1985) of several sandstone samples, using the same cubic lattice network model as pore structure, which may appear surprising at first considering that the range of pore diameters sizes vary widely from one rock to another, becomes apparent.

Finally, it is established that the permeabilities of most sandstones fall in zone II of the conductance envelope (Fig. 7), and that the permeabilities predicted by the Kozeny-Carman formulas are valid within more or less a factor of three of the observed values. Consequently, even though the complete pore space system of most sandstones is strictly speaking inhomogeneous, the hydraulically active or 'principal' network approaches homogeneity. As the rock 'principal' pore network becomes more and more inhomogeneous, the conductance plot shows that the Kozeny-Carman formulas become less and less applicable. For a very inhomogeneous 'principal' network, Fig. 7 shows that the critical path analysis can be applied within limits. We are in the process of obtaining the conductance envelope for different pore distribution functions, but we do not anticipate that the type of distribution will have a strong effect on the described behaviour.

8. Acknowledgements

This research was supported by the U.S. Department of Energy through the Assistant Secretary for Fossil Energy, Bartlesville Project Office, Advanced Extraction Process Technology (AEPT), under contract No. DE-AC22-89BC14475, with the University of California at Berkeley. Additional funding was provided by the Director, Office of Energy Research, Office of Basic Energy Sciences, Engineering and Geosciences Division, under contract No. DE-AC03-76SF00098 with the Lawrence Berkeley Laboratory. Thanks are due to Christine Doughty and Robert Zimmerman of Lawrence Berkeley Laboratory for carefully reviewing this note.

References

[1] Ambegaokar, V., Halperin, B.I., and Langer, J.S. 1971. Phys. Rev. B 4 (8), p.2613.

[2] Batra, V.K. 1973. An experimental investigation of the structure of porous media and its relation to oil recovery. Ph.D. Thesis. University of Waterloo.

[3] Berryman, J.G., and Blair, S.C. 1987. Kozeny-Carman relations and image processing methods for estimating Darcy's constant. J. Appl. Phys. 62 (6), p.2221.

[4] Carman, P.C. 1941. Capillary rise and capillary movement of moisture in fine sands. Soil Sci. 52, p.1.

[5] Chatzis I., and Dullien, F.A.L. 1985. The modeling of mercury porosimetry and the relative permeability of mercury in sandstones using percolation theory. A.I.Ch.E. 25 (1), p.47.

[6] Efros, A.L. 1986. Physics and geometry of disorder. Mir publishers, Moscow.

[7] Kirkpatrick, S. 1971. Classical transport in disordered media: Scaling and effective-medium theories. Phys. Rev. 27 (25), p.1722.

[8] Kirkpatrick, S. 1973. Percolation and conduction. Rev. Mod. Phys. 45 (4), p.574.

[9] Scheidegger, A.E. 1974. The Physics of Flow through Porous Media. University of Toronto Press.

[10] Schlueter, E.M. 1993. Predicting the transport properties of sedimentary rocks from microgeometry. Lawrence Berkeley Laboratory Rep., LBL-33830, Berkeley, Calif.

[11] Schlueter, E.M., Witherspoon, P.A., Cook, N.G.W., and Myer, L.R. 1994. Relative Permeability and the microscopic distribution of wetting and nonwetting phases in the pore space of Berea sandstone. Lawrence Berkeley Laboratory Rep., LBL-34109, Berkeley, Calif.

[12] Schultze, K. 1925a. Kapillarität, verdunstung, und auswitterung. Kolloid Ztschr., 36, p.65.

[13] Schultze, K. 1925b. Kapillarität und Benetzung. Kolloid Ztschr., 37, p.10.

LAWRENCE BERKELEY LABORATORY
UNIVERSITY OF CALIFORNIA
TECHNICAL INFORMATION DEPARTMENT
BERKELEY, CALIFORNIA 94720